Technical Paper by Y. Liu, J.D. Scott and D.C. Sego

GEOGRID REINFORCED CLAY SLOPES IN A TEST EMBANKMENT

ABSTRACT: A 12 m high geogrid reinforced cohesive soil test embankment with 45° side slopes has been built near Devon, Alberta, Canada. The embankment has four test sections: three are reinforced with different geogrids, and one section is unreinforced. The test sections were instrumented with strain gauges and inductance coils on the geogrids) and extensometers, inclinometers and piezometers in the soil. The design, construction and instrumentation of the test embankment is described. Field measurements, taken from the slopes over a seven year period during and after construction, are presented and discussed. The development and the distribution of geogrid strains, soil deformations and pore pressures are presented to show the performance of the reinforced cohesive soil slopes.

KEYWORDS: soil reinforcement, geogrids, slopes, field measurements, clay.

AUTHORS: Y. Liu, Project Engineer, Golders Associates Ltd., 1011-6th Avenue, S.W., Calgary, Alberta, T2P 0W1, Canada, Telephone: 403/299-5600, Telefax: 403/299-5606. J.D. Scott, Professor, Emeritus, and D.C. Sego, Professor, Department of Civil Engineering, University of Alberta, Edmonton, Alberta, T6G 2G7, Canada, Telephone: 403/492-2636, or 403/492-2059, Telefax 403/492-8198.

PUBLICATION: *Geosynthetics International* is published by the Industrial Fabrics Association International, 345 Cedar St., Suite 800, St. Paul, MN 55101, USA, Telephone: 1/612-222-2508, Telefax: 1/612-222-8215. *Geosynthetics International* is registered under ISSN 1072-6349.

DATES: Submitted 28 December 1993, accepted 31 January 1994. Discussion open until 1 September 1994.

REFERENCE: Liu, Y., Scott, D.J. and Sego, D.C., 1994, "Geogrid Reinforced Clay Slopes in a Test Embankment," *Geosynthetics International,* Vol. 1, No. 1, pp. 67-91.

INTRODUCTION

Geotextiles and geogrids have been used extensively in soil reinforcement for the past few decades. The use of soil reinforcement typically reduces cost of construction, increases tolerance of the soil structures to ground movement and increases the feasibility of soil structures which are difficult to construct using conventional methods due to poor soil conditions or limited right of way. Three types of soil structures in geotechnical engineering are reinforced: retaining walls, slopes, and embankments on soft foundations. For a reinforced embankment on a soft foundation, a layer of reinforcement is usually placed at the base of the embankment to carry part of the horizontal load from the embankment and to prevent failure in the soft foundation soils. For a reinforced wall or a slope, reinforcing layers are placed within the backfill materials. Other than the geometrical difference, these two types of reinforced soil structures (walls and slopes) can be distinguished by the tensile force distribution in the reinforcement. For a typical reinforced wall, the reinforcement is attached to rigid facing units and, therefore, the maximum tensile force in the reinforcing element generally occurs at the surface of the wall. For a reinforced slope, the reinforcement is usually unconnected at the face and the tensile force in the reinforcement is zero at the slope surface as reported by Fannin and Hermann (1990). In addition to these two types of structures, there is another type of reinforced soil structure which has characteristics of both reinforced walls and slopes. In this type of structure, which can be vertical or sloped, the reinforcement is either connected to flexible facing units, such as metal meshes, or is wrapped around the compacted backfill. The location of the maximum tensile force in the reinforcing layer depends on the rigidity of the facing units and the horizontal movement within the backfill.

For reinforced slopes, deformation and stability are the two main concerns. An accurate assessment of deformation in a reinforced slope can only be achieved through a stress-deformation analysis, such as a finite element analysis. Stability of a reinforced slope, on the other hand, can be evaluated using either a limit equilibrium method or a stress-deformation analysis. Limit equilibrium methods are still the most common analytical approaches in recent design practices for reinforced slopes. Worldwide case records of reinforced soil structures indicate that the current design methods are conservative, as reported by Mitchell (1987). The conservatism comes from uncertainties in the following:

- stress-deformation characteristics of reinforced slopes and load distributions within the soil and the reinforcement;
- failure modes of reinforced slopes and suitable corresponding limit equilibrium methods;
- reinforcement mechanisms in slopes reinforced with geosynthetics;
- mobilization of the shear strength in the soil and the definition of the factor of safety in a reinforced slope;
- mobilization of the tensile strength in the reinforcement and performance criteria of reinforcing materials;
- reinforcement force orientation and its incorporation in the stability analysis;

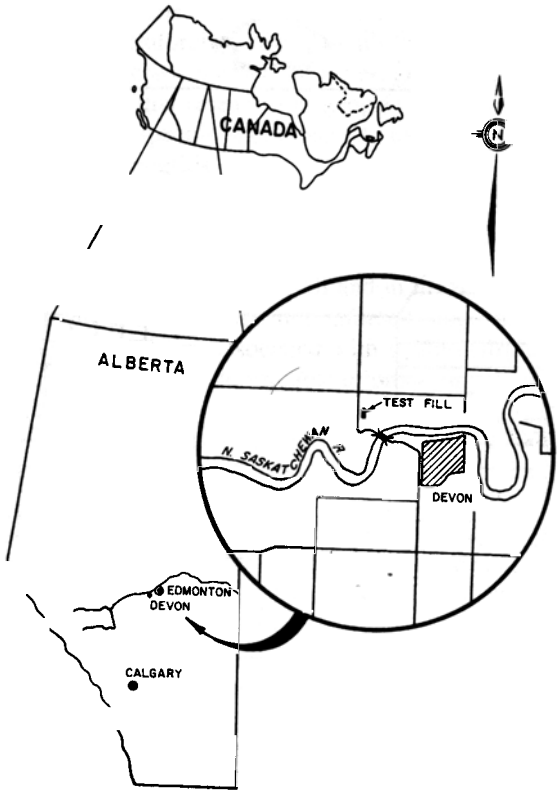

Figure 1. Location of test embankment.

- interaction between the soil and the reinforcement and the strain compatibility; and
- deformation patterns of reinforced soil slopes.

To obtain rational and economical designs of reinforced slopes, a good understanding of the above aspects is required. Well instrumented full scale tests are the most appropriate approaches to fulfil this requirement. To achieve a better understanding of the reinforcement mechanism in a geogrid reinforced cohesive soil slope and to accumulate experience for both analytical and practical purposes, a test embankment, 12 m high with 1:1 side slopes, was built near Devon, Alberta, Canada (Figure 1). The test fill has four sections, three reinforced with different types of geogrids, uniaxial, geogrids (Tensar SR2), rectangular geogrids (Signode TNX5001) and square geogrids (Paragrid 50S), and one unreinforced section, as shown in Figure 2. Locally available silty clay was used as the fill material and three layers of geogrids were installed in each reinforced test section as the primary reinforcement.

This paper presents the properties of the soils and the reinforcing materials, the details of the construction and the instrumentation of the test embankment, and the field measurements from the unreinforced section and two reinforced sections. Field measurements taken over a three year period, during and after construction, were reported earlier by

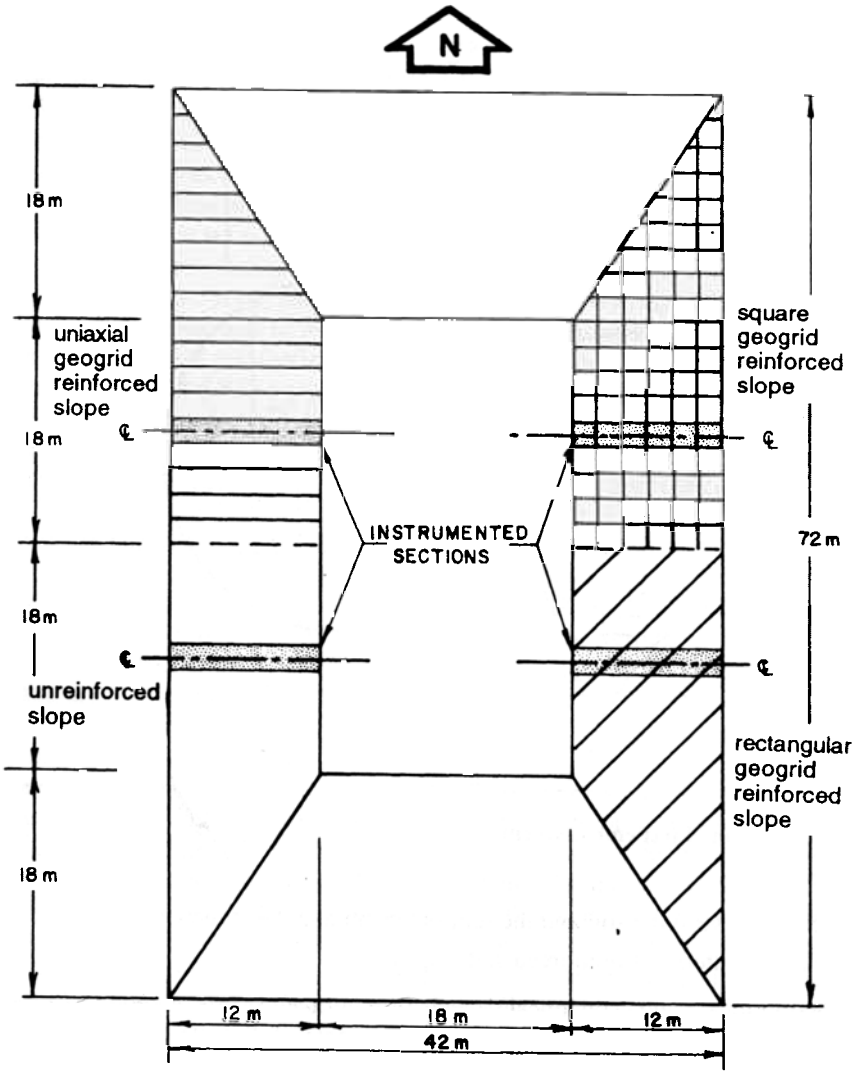

Figure 2. Plan view of test embankment.

Sego et al. (1990) and are extended here to a seven year period. Due to some defects in the square geogrid materials installed in the test embankment, as will be discussed later, the strains which developed in these geogrids are highly localized and the overall behaviour of the square geogrid reinforced slope is similar to the unreinforced slope. Hence, the performance of that reinforced slope will not be discussed separately.

Several instrumented slopes for research purposes have been reported in the literature, for example, by Fannin and Hermann (1990), Bassett and Yeo (1988) and Rimoldi (1988). Strains in the reinforcement and deformations of the slope surfaces were the most common field measurements. Soil deformations within the slopes were monitored

in some cases. Occasionally, tensile loads in the reinforcement were measured to compare the field stiffness of the reinforcing material with the stiffness obtained from laboratory tensile tests. In the majority of cases, however, geogrids were used to reinforce granular materials. Therefore, this research on geogrid reinforced clay slopes in the Devon test embankment, has a specific significance to the understanding of how cohesive soils are reinforced with geogrids.

The major objectives of this research were to determine how individual geogrid layers reinforce a mass of cohesive soil and to measure the stress transfer from the soil to the geogrids within the embankment. The studies have been carried out through a comparison between the strain distribution in the soil and in the reinforcement and a comparison between the strain profiles in the unreinforced slope and in the reinforced slopes. Load distributions, which are associated with strain distributions, within both the fill and the reinforcing layers provide valuable information related to reinforcement location, spacing and layout. Secondary objectives of the research were to compare the performance of three different geogrid materials, to evaluate the field performance of the compacted fill and its foundation soils, and to evaluate the procedures used to construct geogrid reinforced slopes.

High strength and high modulus geogrids in a reinforced slope will modify the magnitude and distribution of the lateral deformation and thus the stress distribution in the slope. Measurements of the stress transfer between the soil and the geogrids during the construction of the embankment were an important aspect of this study. Thus, the test slopes were designed with a low factor of safety to develop lateral strain in the soil which would mobilize the tensile resistance of the geogrids. To ensure that measurable lateral strains would occur and to ensure that each reinforcing layer would act independently, only three primary reinforcing layers at a 2 m vertical spacing were installed in the bottom half of the test fill as shown in Figure 3. This small number of geogrid layers was chosen to increase the efficiency so that both the local stability and overall stability of the slope were achieved while allowing significant soil deformation to occur. The length of the primary reinforcing layers was determined such that there was

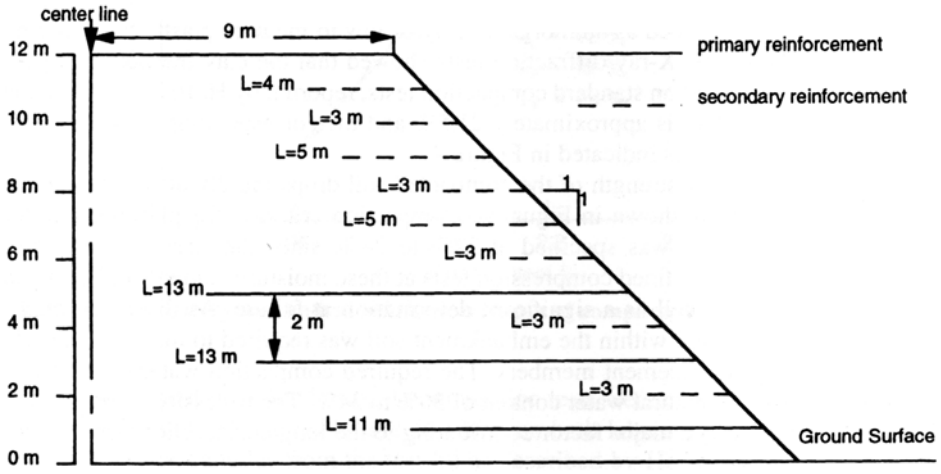

Figure 3. Geogrid layout in reinforced sections.

sufficient embedment beyond the predicted overall failure surface to prevent pullout of the reinforcement.

DESCRIPTION OF THE FIELD TEST

Properties of Foundation Soils, Fill and Geogrids

The properties of the fill and foundation soils in the test embankment were studied by Hofmann (1989). The embankment was founded on and constructed of glaciolacustrine sediments. The top 4 m of the foundation soil consists of a soft silty clay at an average natural water content of 32% (liquid limit of 37% and plastic limit of 24%). The dominant particle size of the soil is silt while the clay sizes are only 10 to 20%. This uppermost layer of the foundation soil is underlain by 2 m of a stiffer sandy, silty clay. Below the 6 m depth, a fine, very dense 1.5 m thick layer of grey sand exists and this is underlain by a hard clay till. The ground water table was 5 m below the ground surface. From the geological profile of the surficial sediments, it was obvious that the deformation of the foundation soils due to the construction of the test embankment would occur mainly in the glaciolacustrine deposits. Therefore, the laboratory studies were focused on the uppermost silty clay.

Consolidated undrained triaxial compression tests with pore pressure measurements were conducted on Shelby tube samples and block samples of the silty clay from the foundation. Most specimens exhibited either a hyperbolic or an elastic-perfectly plastic stress-strain behaviour. The pore pressure during shearing was positive indicating a tendency of the soil to contract during shear. Skempton's pore pressure parameter at failure, A_f, tended to increase from 0.1 under a low effective confining stress to 0.83 under a confining stress of 275 kPa. The tests indicated an effective friction angle of 27° and an effective cohesion of 20 kPa.

To meet the design requirement that the fill soil deform sufficiently to induce strain in the geogrids, a relatively soft silty clay in the test site area was selected as the material to construct the embankment. The soil is composed of 25% sand, 50% silt and 25% clay sizes. The liquid limit and plastic limit of the fill soil are 42% and 18% respectively; the soil is described as an inorganic clay of low to medium plasticity according to the Atterberg limits. X-ray diffraction tests showed that the clay fraction is largely montmorillonite. Based on standard compaction tests, reported by Hofmann (1989), the optimum water content is approximately 21.5% and the corresponding maximum dry density is 1,600 kg/m^3 as indicated in Figure 4.

The undrained shear strength of the compacted soil drops rapidly at water contents above the optimum as shown in Figure 4. Compaction criterion for placement water content for the test fill was specified at 22% to 24%, since the stress-strain curves obtained from the unconfined compression tests at these moisture contents indicated an adequate strength as well as a significant deformation at failure. As discussed previously, such deformation within the embankment soil was required to mobilize the tensile force in the reinforcement members. The required compaction water content was well below the soil's natural water content of 30% to 34%. The necessity to dry the soil before placement was a major factor contributing to the long construction period.

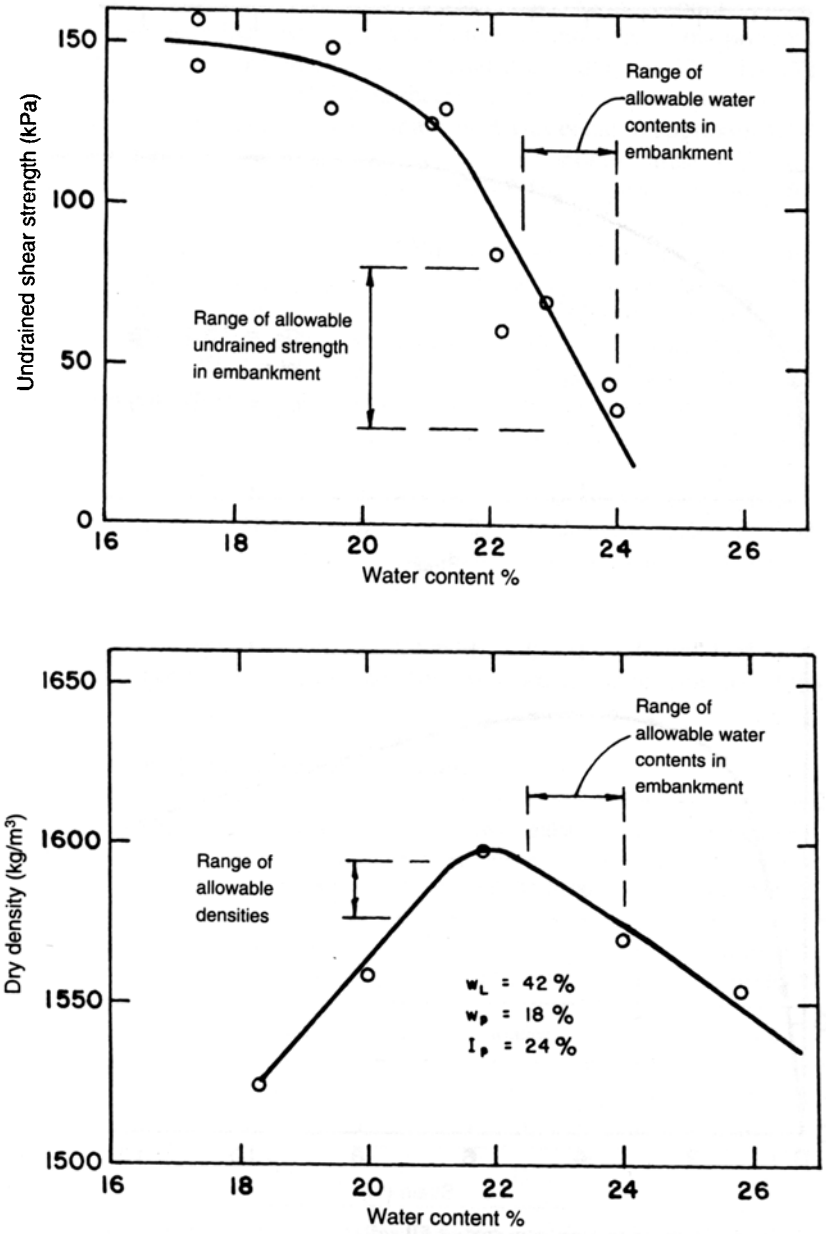

Figure 4. Dry density and undrained shear strength of compacted fill soil.

Unconsolidated undrained triaxial compression tests were carried out, under confining pressures of 0, 80, 160, 240 and 360 kPa, on both laboratory compacted samples and Shelby tube samples from the test fill as described by Hofmann (1989). An average undrained shear strength of 76 kPa was obtained. Consolidated undrained triaxial

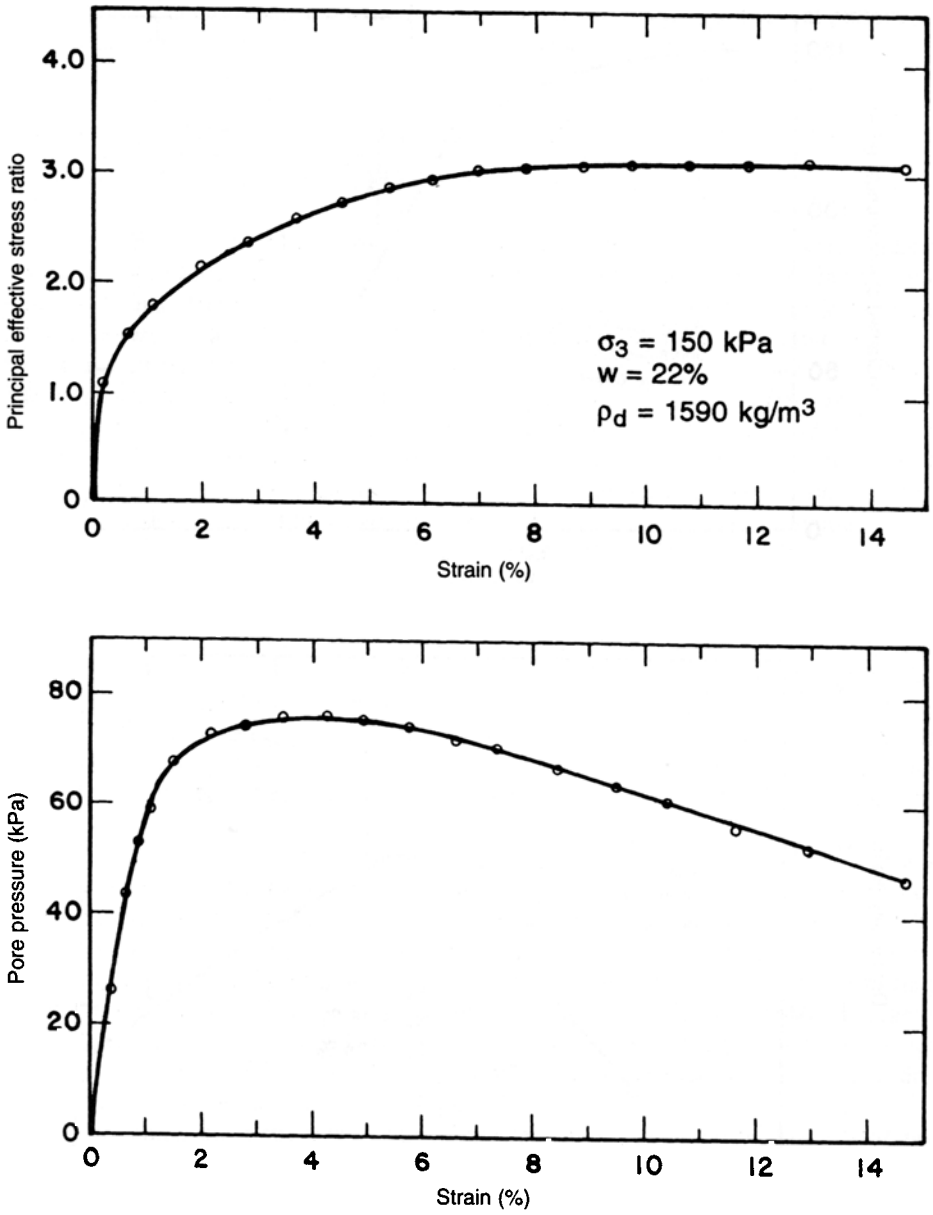

Figure 5. Triaxial shear test on compacted fill soil.

compression tests with pore pressure measurements were also conducted on the compacted fill soil. The soil was compacted at water contents between 22% and 24% and the specimens were consolidated under confining pressures of 75, 150, 200 and 300 kPa prior to shearing. Typically, the soil exhibited a strain strengthening behavior. The

stress-strain curves show a high tangent modulus and, beyond about 2% strain, the stress rises slowly with increasing strain to failure. In most cases, the principal effective stress ratio reached a maximum value at axial strains of about 12%. The pore pressures, however, rapidly increased during shearing, reaching a maximum at 4% strain as shown in Figure 5. The pore pressure parameter A was equal to approximately 0.50 at high confining stresses and equal to about 0.16 at low confining stresses. The tests gave an average effective friction angle of 28° and an effective cohesion range from 8 to 14 kPa.

Three types of high tensile strength geogrids were used as primary reinforcing materials in the test slopes. The physical properties of the geogrids are summarized in Table 1 and the results of wide strip tensile tests are shown in Figure 6. It is realized that the behavior of the geogrid materials is strain rate dependent. The wide strip tensile tests, therefore, were conducted not to simulate the field loading condition. Instead, they were to compare the different geogrid materials at the same loading condition. The uniaxial grids are desirable for plane strain applications, such as reinforced slopes and walls. The rectangular grids were made from polyester strips. The longitudinal and latitudinal strips were ultrasonically bonded to one another forming the junctions as described by Koerner (1990). Similar to the uniaxial grids, the rectangular grids are desirable in plane strain applications. The square grids consist of high-tenacity polyester filaments held together by a polypropylene sheath. At the joints between the longitudinal and latitudinal ribs, the contacting polypropylene sheaths are melt-bonded to one another. During laboratory tests on the square grids supplied and placed in the test slope, it was found that some of the high strength filaments in the tension members were weakened or damaged at the inter-

Table 1. Physical properties of geogrid materials.

Geogrid Structure	Uniaxial	Rectangular	Square
Product	Tensar SR2	Signode TNX5001	Paragrid 50S
Type of polymer	high density polyethylene	polyester	polyester polypropylene
Junction	planar	welded	welded
Mass per unit area (g/m^2)	930	544	530
Open area (%)	55	58	78
Aperture size (mm)	MD 99.1 CMD 15.2	MD 89.7 CMD 26.2	MD 66.2 CMD 66.2
Thickness (mm)	T 1.27 A 4.57	T 0.75 J 1.5	T 2.5 J 3.75
Color	black	black	yellow

Notes: MD: machine direction; CMD: cross machine direction; T: Longitudinal (tension) member; A: Latitudinal (anchor) member; J: joint.

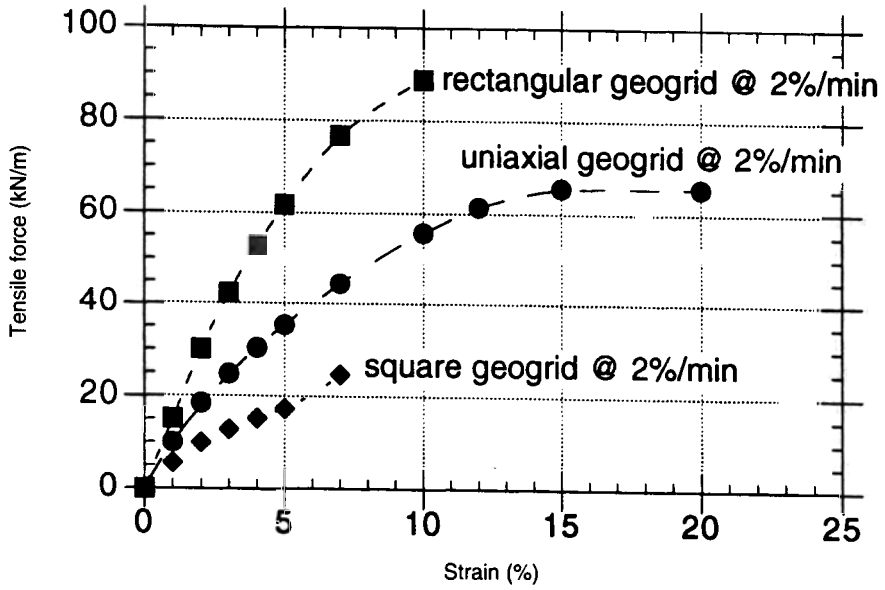

Figure 6. Wide strip tensile test results.

sections of the grids. This damage was most likely caused by overheating of the polypropylene sheath during the welding process.

As well as the primary reinforcing materials mentioned above, geogrids were used in the three reinforced sections of the test fill as secondary reinforcing materials to provide additional reinforcement against shallow slope failures and failures at the top of the steep soil slopes from compaction equipment during the construction process.

Construction and Field Observations of the Test Slopes

The construction of the test embankment commenced in the summer of 1986. Prior to the construction, the foundation instrumentation was installed to establish zero reference values. The construction of the test embankment was carried out in three stages. The site and foundation preparation started on 8 June 1986 with stripping of the organic top soil and grading of the site to a horizontal foundation elevation of 702 m. The bottom level of horizontal instrumentation tubes were installed in shallow trenches just below the ground level prior to the placement of the fill soil. On 4 September 1986 (day 0) placement of the embankment soil began. The fill soil was excavated from an adjacent road cut and placed by scrapers, spread using bulldozers and compacted using a four wheel rubber tire compactor. A small bulldozer and a small light compactor were used along the edge of the steep slopes and near the locations of the vertical instrumentation. The fill was usually placed and compacted in lifts varying between 0.15 m and 0.4 m thick. Field density tests (in-situ methods) were conducted and the water content of the fill was monitored for quality control purposes throughout the construction. When the fill height

reached 1 m, the fill was leveled, and the bottom primary reinforcement geogrid layer was stretched into place and held down with soil spikes. Electrical cables were then attached to both types of strain gauges, which had been previously bonded to the geogrids in the laboratory, before the instrumented geogrid sections were shipped to the construction site. A set of strain gauge readings were taken as the initial measurements immediately after the instrumented geogrids were laid out and the cables attached. A 0.3 m lift of fill soil was then placed and compacted on the top of this first primary reinforcing layer and the embankment was constructed in 0.15 m lifts to the 2 m height where horizontal soil instrumentation and a layer of secondary reinforcement geogrids was placed. The fill was then constructed to a height of 3 m, by 23 October 1986, when construction stopped due to the onset of winter conditions. To prevent drying of the clay fill during shutdown, a 0.3 m lift of sand was spread on the fill surface.

The construction of the test fill did not resume until 30 August 1987. The layer of sand was removed and clay fill was placed and compacted in 0.15 m lifts to the 3 m elevation where the second primary reinforcement layer of geogrids was placed. The fill construction was continued to the 4 m height where horizontal soil instrumentation and a layer of secondary reinforcing geogrid was placed and then to the 5 m height where the third primary reinforcement layer was placed. The fill height reached 6 m at the end of the second construction season on 3 November 1987.

The construction of the test fill continued during the following summer. The top 6 m of soil was placed to reach the 12 m design height on 29 October 1988. Six layers of secondary reinforcing geogrids at 1 m vertical spacing were placed during the 1988 construction season. Due to rainy weather and limited construction time, the top 6 m of the fill soil was placed and compacted wet of the design water content using larger lifts than were used in the bottom 6 m of the test embankment. The water content of the top 6 m of the embankment was estimated to be about 3 to 5 % higher than in the bottom 6 m of the embankment.

There were several uncontrollable variables during the construction of the test embankment. Firstly, due to rain, the water content of the soil varied slightly. Secondly, the fill soil was often too wet and drier soils had to be added and mixed with the wet soil. Finally, because of the steep side slopes, the compaction of the soil along the edges was lower than that of the soil in the center. The above variables influenced the consistency and uniformity of the soil properties throughout the test embankment.

After the construction was completed, erosion control materials were placed on the slopes and top of the test embankment during the fall of 1988 and the spring of 1989. During the rainy season in the early summer of 1989, some surface movements of the slope occurred. The soil movements were mainly in the bottom 6 m of the embankment and were located about 0.5 m deep and parallel to the slope surface. The horizontal extensometer and inclinometer tubes at the ground level and at the 2 m level were covered by the slope debris. During the summer of 1990, similar but more severe surface soil movements occurred. Although the depth of the movements remained about 0.5 m, the movements migrated up the slope surface to the 8 or 9 m level and more soil was involved. Hand and machine excavation was used to regain access to the buried instrumentation after the surface sloughing. Surface movements again occurred during the summer of 1991 and more debris accumulated at the toe of the slopes.

These surface movements appeared to be related to softening within the silty clay soil caused by cyclic freeze-thaw which took 2 to 3 years to develop. When freezing

penetrated into the soil, ice lenses likely formed parallel to the slope surface. Upon thaw, the shear strength of the soil decreased while the permeability of the soil parallel to the slope surface increased, which provided conduits for water infiltration during the subsequent rainy periods. As a result, the uppermost 0.5 m of soil sloughed down the slopes. Both the primary and secondary reinforcing geogrids were unable to prevent this soil movement as were the surface protection and erosion control materials. Since the summer of 1991, vegetation cover on the slopes has matured and surface soil sloughing has not been significant.

Some minor instabilities in the unreinforced slope have been observed. In the summer of 1989, tension cracks were noticed at the crest of the unreinforced slope. The cracks were several centimeters wide and several meters long, parallel to the crest. Tension cracks were also observed on the slope surface about 1 to 2 m below the crest. In July 1989, the extensometer access tube at the 4 m level became blocked at a location about 4 to 5 m from the slope surface following heavy rainfall. During the summer of 1990, the tension cracks at the crest of the unreinforced slope became wider and more cracks developed on the top surface behind the crest. At the same time, the tension cracks on the slope surface became longer and wider. In May of 1991, after a heavy rainfall, a shallow soil movement occurred in the unreinforced slope. A back scarp could be seen on the slope surface about 1 to 2 m below the slope crest as can be seen in Figure 7. A series of tension cracks parallel to the crest were observed on the top of the fill behind the crest. The maximum width of the cracks was about 10 cm and the deepest crack was about 2 to 3 m behind the crest of the slope. No similar instabil-

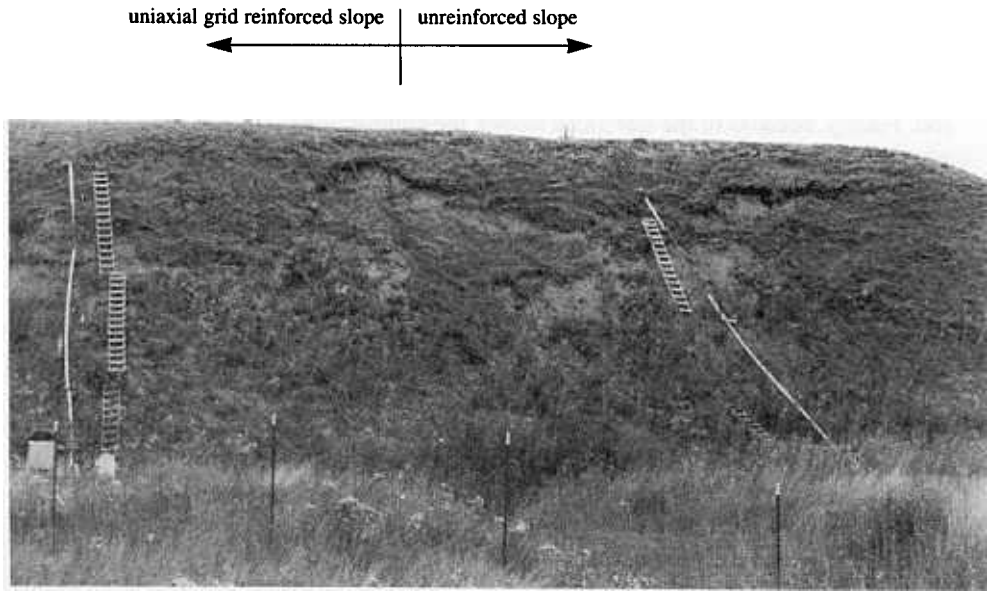

Figure 7. Shallow failure in unreinforced section.

ities were observed in the reinforced sections and since 1991 the unreinforced slope has had little additional movement.

Instrumentation

Extensive instrumentation was installed to measure the performance of the foundation, the fill soil and the geogrids as shown in Figure 8. The main purpose of the instruments was to indicate the overall deformation of the embankment and the foundation soils, the interaction between the soil and the geogrids, and the pore pressure response throughout the test embankment during and subsequent to the construction. Strain distributions in different sections and the localizations of the deformations in the soil and the reinforcement provide indications on load transfer from soil to reinforcement and indications on failure modes of the reinforced slopes. Moreover, field measurements, such as, tensile strains in the reinforcement, soil deformations and pore pressures within the slopes, are valuable input data for subsequent numerical analyses and finite element modelling of the reinforced slopes.

The strains in the geogrid were monitored using inductance coil sensors (as strain gauges) and electrical wire resistance (EWR) strain gauges. The strain gauge positions were at 0.5 m and 1.0 m and then at 1 m intervals from the slope surface. Pairs of inductance coil sensors were attached by plastic bolts placed through the center of adjacent latitudinal members in the geogrids. The coils monitor the displacements between the two sensors and can measure strains beyond deformations at which the EWR strain gauges would fail. Calibration inductance coils were also installed to check and correct for uncertain variations in the field readings such as readout box sensitivity and temperature change in the soil. EWR strain gauges were installed at each instrumented position on the top and the bottom of a longitudinal member of the geogrid to measure the small strains induced in the geogrid. Each gauge was bonded to the geogrid using epoxy and then was waterproofed. A thermocouple was placed at each instrumentation position to allow corrections for the influence of temperature variations. Calibrating EWR strain gauges were also installed in the test fill at 0.5, 1 and 5 m from the slope surface to aid in correcting for temperature variations. The global strains recorded by the inductance coil sensors and the local strains from EWR gauges were used to calculate the loads induced in the geogrids as the embankment soils deformed.

Movements of the soil in the fill and the foundation were monitored using extensometers and inclinometers, installed both horizontally and vertically in the fill and vertically in the foundation soils. The measurements from these instruments indicated the soil movements during and after the construction of the embankment.

Horizontal extensometers and inclinometers were placed at the 0, 2, 4 and 6 m heights in the embankment. The multipoint magnetic horizontal extensometers measured horizontal displacements of the soil between adjacent magnets approximately two meters apart. The displacements were then converted to average horizontal strains of the soil between the magnets. Horizontal Sinco telescoping inclinometers measured the vertical deflections every 0.6 m from one side of the test embankment to the other. The measured vertical deflections, together with measurements of vertical extensometers and ground surveys, provided profiles of settlements at the different instrumentation

levels. Unfortunately, all instruments at the 6 m level were damaged shortly after their installation during the 1988 construction season.

Vertical extensometers and inclinometers were installed beneath the toe and the crest of the slope at each test section of the embankment. The vertical extensometers measured settlement in the fill and the foundation soils. The deepest extensometer magnet was placed 12 m below the ground surface in the stiff till, to serve as a datum. The vertical inclinometers measured horizontal movement of the fill and the foundation soils, in directions parallel and normal to the slope. No field readings were available from the vertical instruments beneath the crest of the slopes in all four sections of the test fill after the 1988 construction season due to unrepairable damage.

The pore pressure response of the fill soil and the foundation during construction and during the subsequent consolidation period was monitored using pneumatic piezometers. A total of 56 Sinco pneumatic piezometers were installed within the fill and the foundation soils at the four sections of the test fill. Their locations are shown in Figure 8.

FIELD MEASUREMENTS

Strains in Geogrids

Strains in the geogrids were measured by electric wire resistance (EWR) strain gauges and inductance coils on the twelve instrumented geogrids. A pair of EWR strain gauges was installed at 96 instrumentation locations and they failed at only 8 locations during the 7 years of construction and operation. The inductance coils also failed at only 8 locations out of a total of 87 pairs of inductance coils.

The EWR strain gauges measured the tensile strains developed in the longitudinal members (tension members) of the geogrids while the inductance coils measured the strains between adjacent latitudinal members. If the geogrids deform uniformly, the strains given by the two different measurements should be the same. As shown in Figure 9, for example, the distributions of the geogrid strains from the two types of measurements are similar; the magnitudes of the strain, however, are considerably different. From analysis of the field measurements, it appeared that the EWR gauge strains are more accurate (higher resolution and less uncertainties) than the results from the inductance coils. The strains from EWR gauges also can be directly related to standard tensile tests on geogrids when loads in geogrids are concerned. For these reasons the strains measured using EWR gauges were used as the basis for analyses and the strains from the inductance coils were used in assisting data interpretation.

Figure 9 shows profiles of the tensile strain distribution along the bottom primary reinforcing layer of the uniaxial geogrid at different stages of construction and post-construction consolidation within the embankment. The profiles indicate the changes in magnitude and distribution of the strain as the fill was constructed between day 0 and day 782. Typically, the tensile strain in the reinforcement increases from zero at the slope surface to a maximum at a certain depth and then decreases as the distance from the slope surface increases. The maximum strain developed during the first construction season (day 49) was about 0.5% at 1 m from the slope surface. During the second construction season in 1987 (ending on day 425), only minor increases in the strain occurred. At the end of the final construction stage, day 782, after the top 6 m of the fill

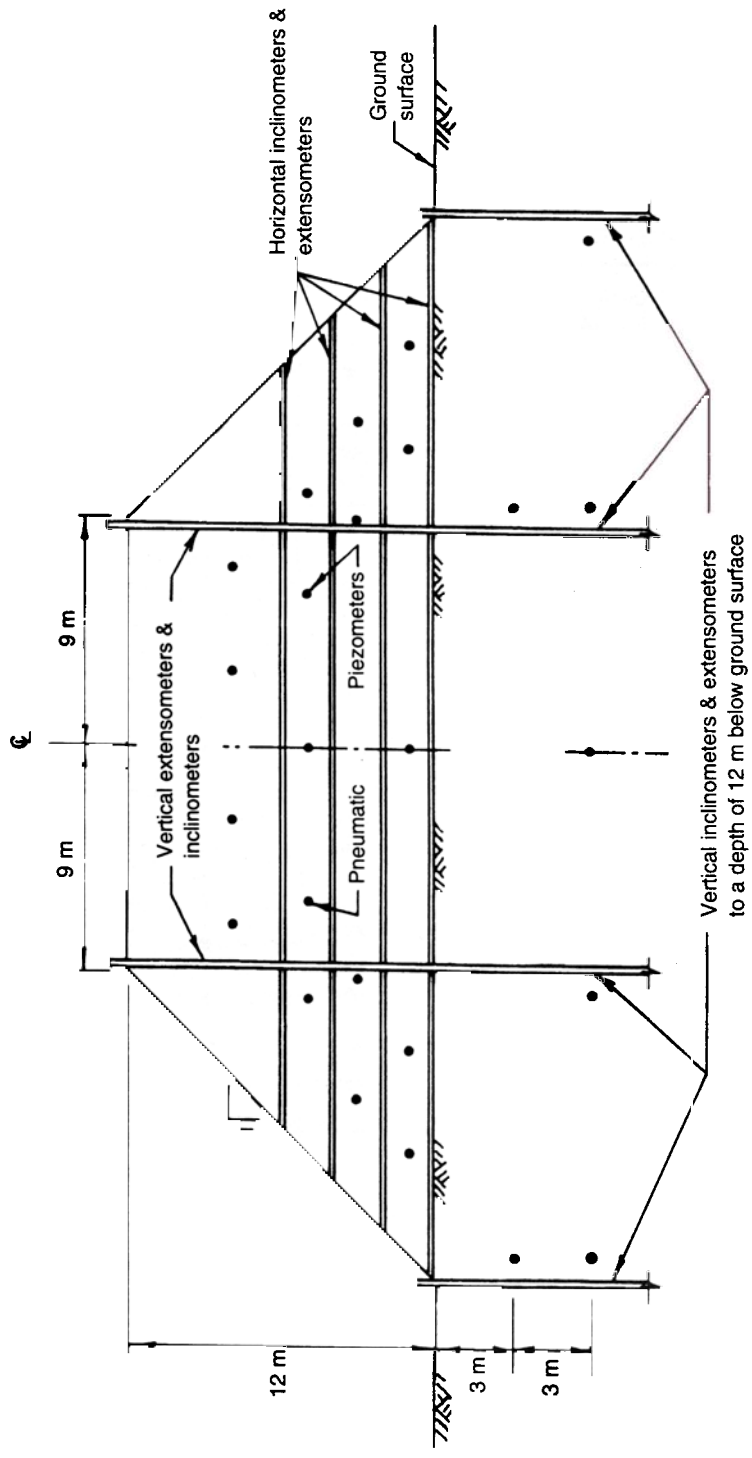

Figure 8. Soil instrumentation in test embankment.

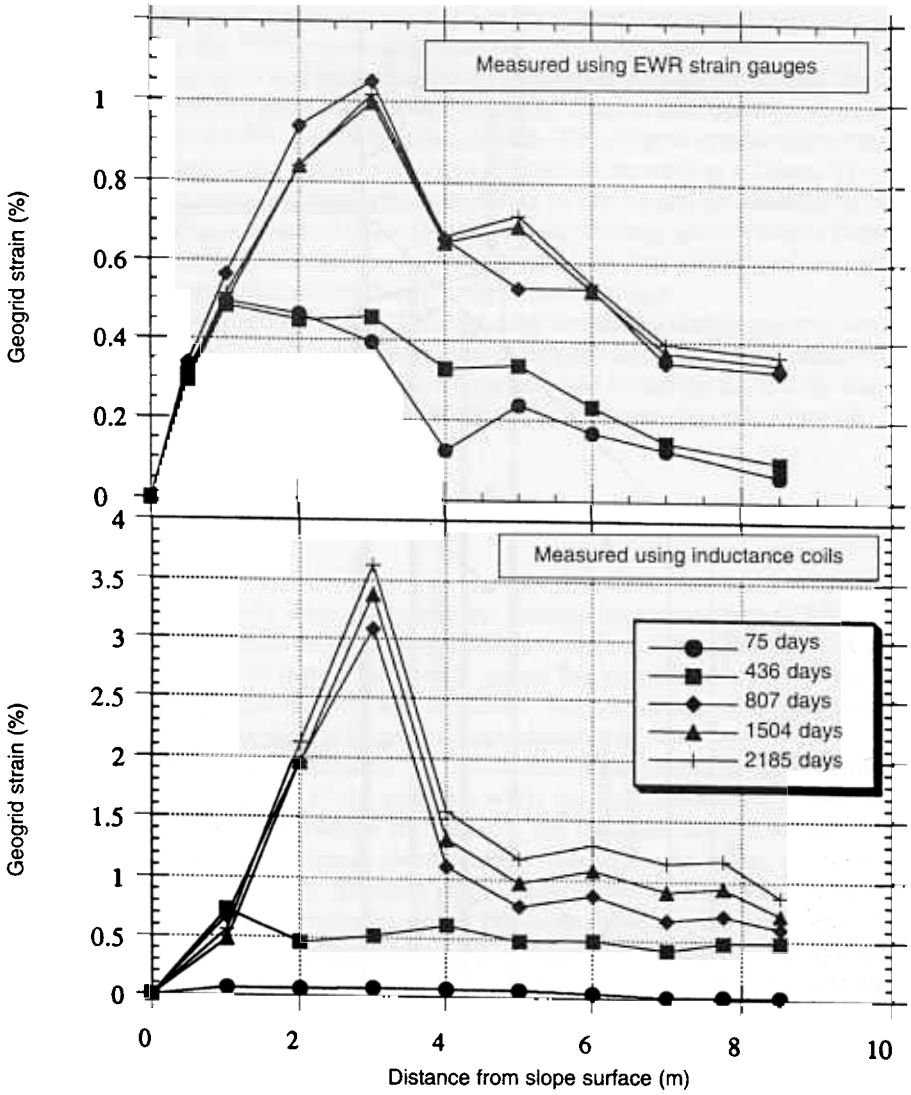

Figure 9. Strain distribution in bottom uniaxial geogrid layer.

was placed, the peak strain had increased to about 1% (from EWR gauges) and had moved to a location 3 m from the slope surface. It remained at this magnitude and location with only minor changes during the subsequent consolidation period. The development of the strain with respect to construction activities at typical locations along that layer of geogrid can also be observed in the strain-time diagrams contained in Figure 10. Tensile strains in other reinforcing layers and other sections had similar variations, in the magnitude and the distribution, and were also correlated with construction and long term consolidation.

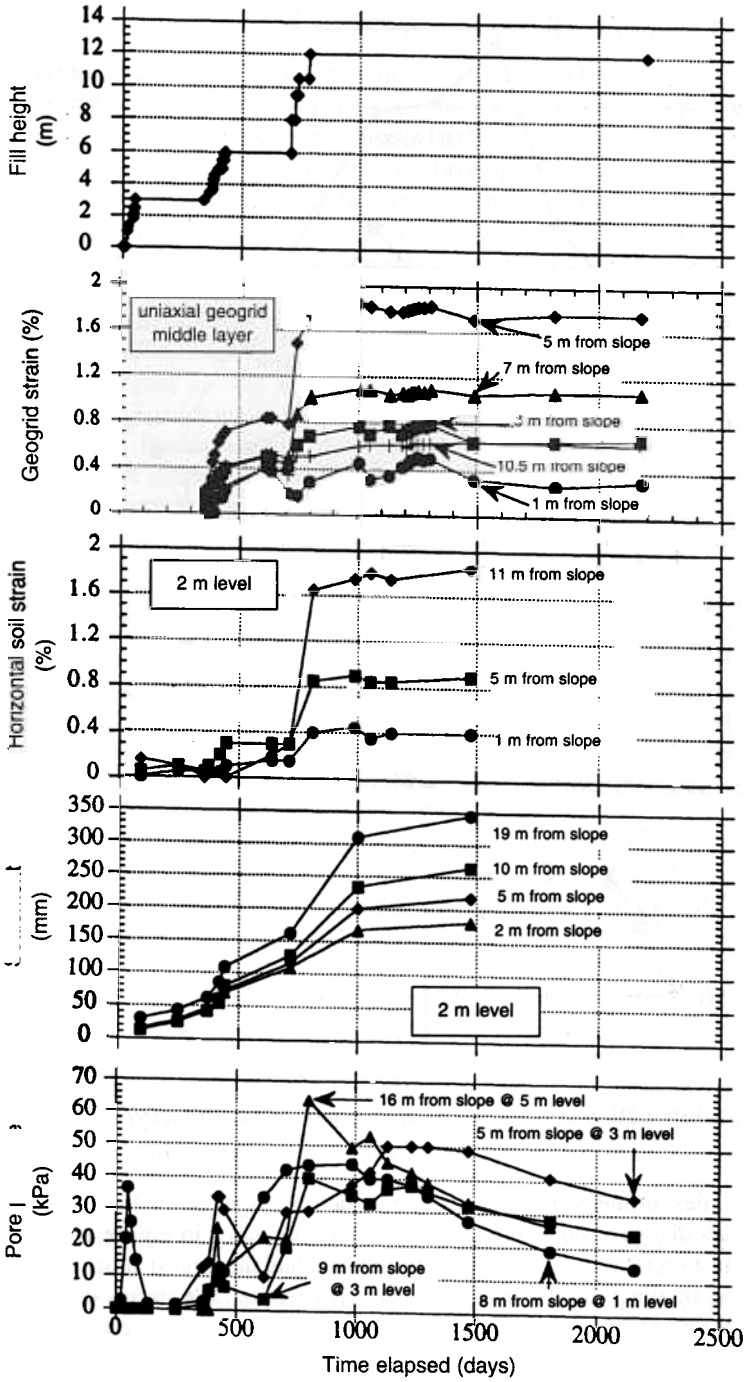

Figure 10. Development of geogrid strains, soil deformations and pore pressures within uniaxial geogrid reinforced slope.

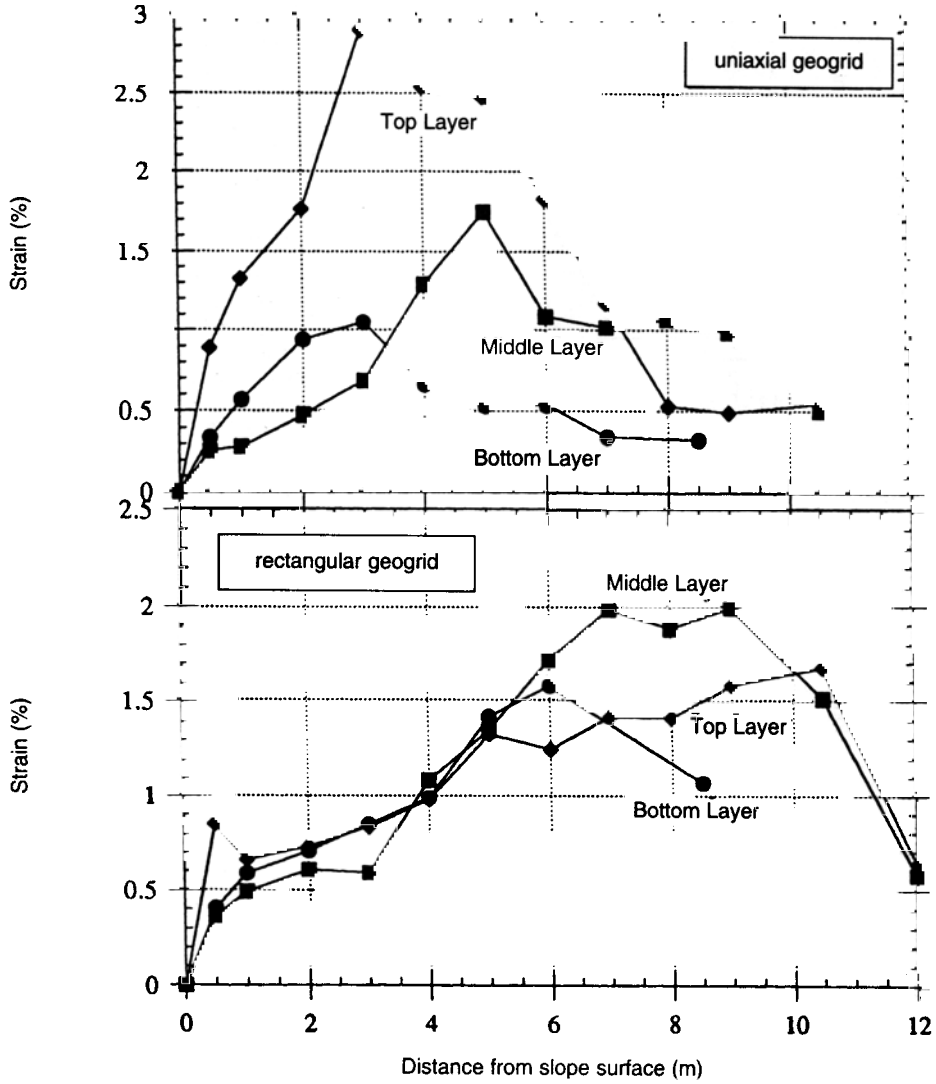

Figure 11. Distribution of geogrid strains at end of construction (807 days)

Strain profiles, at the end of the final construction stage, of the three primary uniaxial and rectangular geogrid reinforcing layers are illustrated in Figure 11. In the uniaxial geogrid test section, the top layer of the geogrid had the largest strain and the bottom layer had the smallest. In the rectangular geogrid section, the strains developed in the three reinforcing layers were of similar magnitudes. It was also noted that the peak strains in the uniaxial geogrids occurred closer to the slope surface than in the rectangular geogrids. The differences in the strain distributions are mainly related to the differences in geometrical and mechanical properties of the two types of geogrids.

Horizontal Movements of the Fill

The horizontal movements of the fill soil were monitored by horizontal magnetic extensometers at different elevations. The measured relative horizontal displacements at 2 m intervals and a reference magnet installed at the center of the fill at each instrumentation level, were interpreted to give the average horizontal strain of the soil between adjacent magnets. Similar to the strains in the geogrids, the horizontal strains of the soil developed following construction of the embankment, as illustrated in the example for the uniaxial geogrid section shown in Figure 10. The horizontal strains of the soil at other sections developed in the same manner.

Profiles of the strain distribution, at the end of the final construction season, in the fill soil at the 0, 2 and 4 m levels in the two reinforced sections and the unreinforced section are shown in Figure 12. The access tubes of the horizontal extensometer and inclinometer at the 6 m level were damaged by construction equipment shortly after their installation in 1988. Profiles at the ground level (0 m level) show the same strain distribution at all three locations. Near the toe of the slope, small negative or compressional strains developed in the soil. From the toe towards the center of the fill, the strains increased gradually. At most locations at the 0 m level, the horizontal strain of the soil was less than 0.5%.

At the 2 and 4 m levels, the strain distribution at the three slopes differed although the magnitudes of the peak strains were similar. In the uniaxial geogrid slope, the strains increased from the slope surface and reached a peak deep into the fill, except for a strain localization 3 m from the slope at the 4 m level, which is an indication of overstressed zones at shallow depths. The strains at the 4 m level were considerably larger than the strains at the 2 m level. In the rectangular geogrid slope, the strains varied rather smoothly at each level with peak strains at 5 to 7 m from the slope surface. The strains at these two levels were nearly the same magnitude. The strains in the unreinforced slope had relatively small magnitudes comparing to the other slopes, except for some localizations. At the 7 m distance on the 2 m level and the 1 and 3 m distances on the 4 m level, the horizontal strains were much larger than at adjacent locations. Also, the strains on the 4 m level were significantly larger than on the 2 m level at most locations.

Horizontal movements of the foundation soils were monitored using vertical inclinometers. Figure 13 shows profiles of the horizontal deflection, in the slope direction, beneath the toe of the slope in the uniaxial geogrid section. Below the -6 m level, the deflection was small and towards the embankment; above the -6 m level, the deflection increased with increasing elevation and reached a maximum at the ground level. Profiles in the other two sections had similar distributions and magnitudes.

Vertical Movement of Soils

Vertical movements of the fill and the foundation soils were monitored using a horizontal inclinometer, a vertical extensometer and by ground elevation surveys. The horizontal inclinometer measured the relative vertical deflection of the casing installed at each instrumented level; the vertical extensometer and ground elevation surveys measured absolute vertical movement at specific points within or on the embankment.

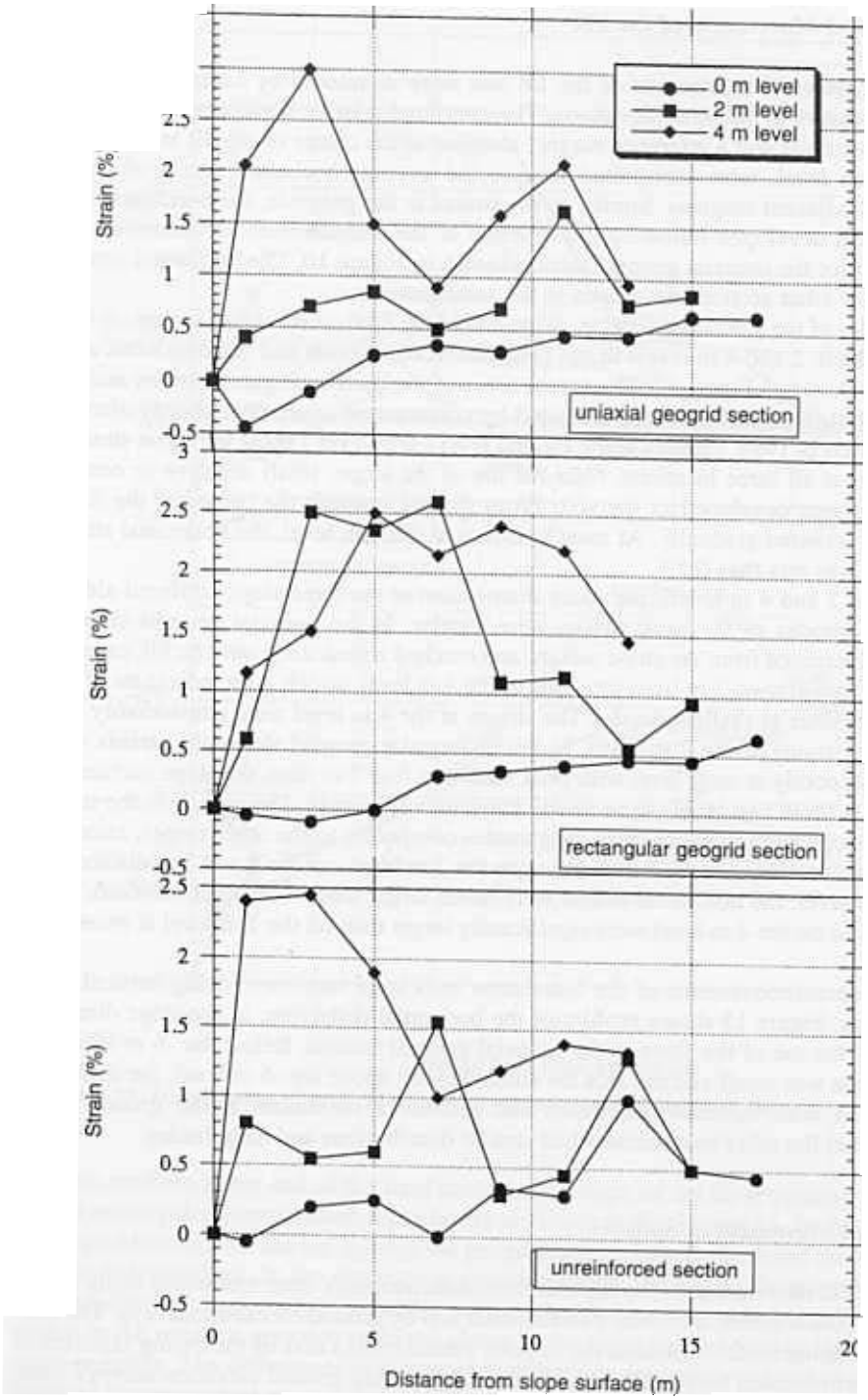

Figure 12. Distribution of horizontal soil strains at end of construction (807 days).

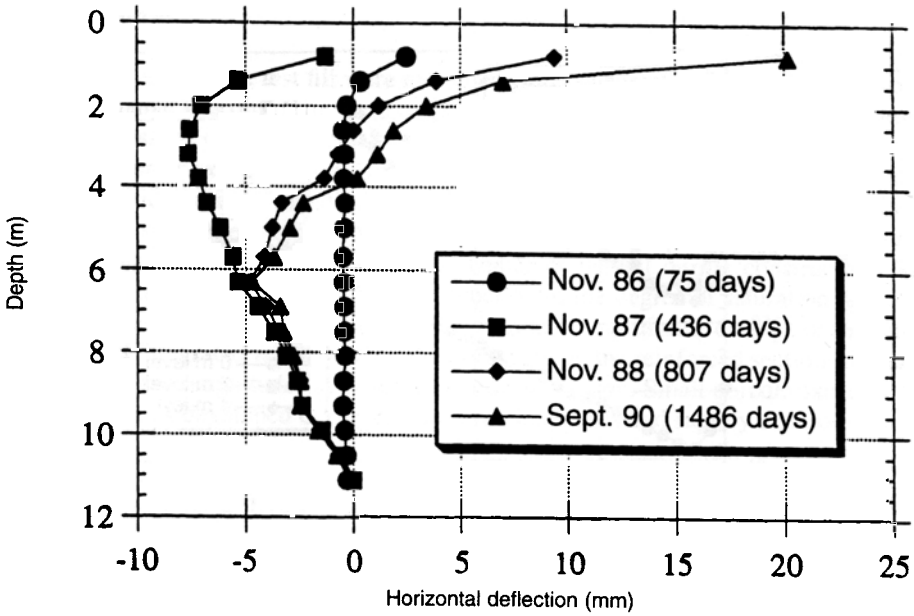

Figure 13. Horizontal deflection in foundation soils beneath toe of uniaxial geogrid of reinforced slope.

Figure 14 shows the settlement profiles, measured six months after the completion of the fill (day 983), at the 0, 2 and 4 m levels in the reinforced and unreinforced slopes. Each profile represents the settlement below the instrumented level after the installation of the inclinometer casing. The development of the settlement, for example at the 2 m level in the uniaxial geogrid section, is illustrated in Figure 10. At all levels in the three sections, the settlement developed coincidentally with construction activities. The settlement occurred rapidly during the construction seasons and continued slowly in the intervening periods.

The settlement profiles in the reinforced and unreinforced sections show different characteristics. In the uniaxial geogrid section, the settlement increased uniformly from the slope surface to the center of the fill at all three levels. In the rectangular geogrid section, localization of the vertical displacements were observed at several locations at the 2 and 4 m levels. The localization can be related either to construction activities or to the development of over-stressed zones. In the unreinforced section, obvious localization of the settlement was found at the 7 m distance at the 2 m level and the 3 and 5 m distances at the 4 m level. The localization of the vertical strains in the unreinforced section is related to the localization of the horizontal strains of the soil at the same levels, as shown in Figure 12, apparently indicating the development of over-stressed zones. The difference in the magnitude of the settlements between the southern part (rectangular geogrid and unreinforced sections) and the northern part (uniaxial and square geogrid sections) of the test embankment mainly occurred in the foundation soils.

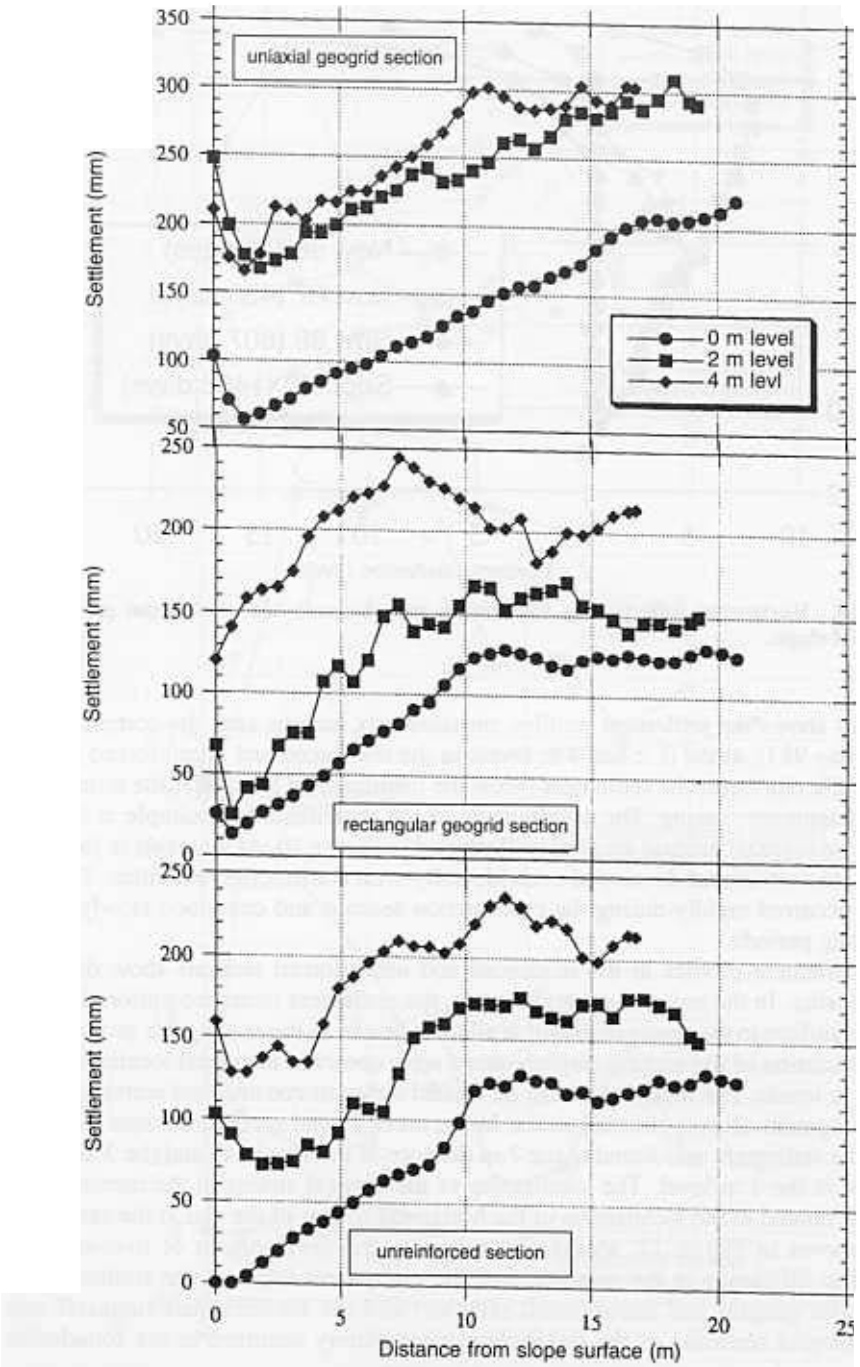

Figure 14. Settlement at end of construction (807 days).

Pore Pressures

Pore pressures in the test fill were measured using pneumatic piezometers. The pore pressure change was directly related to the construction of the test fill. Figure 10 shows the pore pressure development at various locations in the fill at the uniaxial geogrid slope. Pore pressures increased during fill placement and dissipated between and after the construction periods. The dissipation rate after the first construction stage was higher than after subsequent construction periods. At the same elevation, higher pore pressures developed at locations close to the center of the fill during construction. The variation of the pore pressure was also a function of the degree of saturation in the fill soil. The pore pressures at different locations tended to equilibrate during consolidation as pore water migrated within the fill. Pore pressures in the reinforced sections had similar patterns and magnitudes as in the unreinforced section. Small pore pressures in the foundation soils developed during the construction stages and rapidly dissipated.

SUMMARY AND CONCLUSIONS

The performance of the reinforced slopes in the test embankment was monitored by sets of instruments installed in the embankment and on the geogrids. Field measurements showed the mobilization of the tensile resistance in the geogrids, the development of vertical and horizontal displacements in the soils and the variation of pore pressures in the fill and the foundation soils. More details of the field measurements are given by Liu (1992). These measurements from the test embankment provide a better understanding of reinforcement mechanisms, deformation patterns, development of over-stressed zones and possible failure modes of geogrid reinforced cohesive soil slopes. The following observations are summarized from the field measurements:

1. Tensile strains in the geogrids and horizontal soil strains within the reinforced slopes developed during the placement of the fill. There were two distinct phases in the development of the strains and the deformations. During the 1986 and 1987 construction seasons when the fill height was less than 6 m, the strains and the deformations were small and were uniformly distributed. The slopes deformed significantly after the 1988 construction season when the top 6 m of the fill was placed. When the fill height increased to 12 m and the corresponding factor of safety for slope stability of the unreinforced slope was close to unity, the tensile strains increased significantly to a maximum of 2.8% for the uniaxial geogrid and 2.0% for the rectangular geogrid. The development of the strains in the soil and the geogrids was not proportional to the fill height and therefore implies a nonlinear soil stress-strain behavior within the embankment.
2. The tensile strain distribution along the geogrids is similar in all geogrid layers and in all test sections. The strain increased from zero at the slope surface to a maximum and then decreased. The locations of the peak tensile strains in the geogrid material of higher tensile stiffness (rectangular geogrid) were usually deeper within the fill than in the geogrid of lower stiffness (uniaxial geogrid).

3. The distribution of the horizontal soil strains between each instrumentation level is similar to the distribution of the tensile strains in the geogrid layers. The locations of the peak soil strains, however, can be different from the peak tensile strains in the geogrids. In the uniaxial geogrid reinforced section, the locations of the peak soil strains are further from the slope surface than the peak tensile strains in the reinforcement, while in the rectangular geogrid section, the locations of the peak soil strains are similar to those in the geogrid.
4. The vertical distribution of the maximum tensile strains in the 1 m, 3 m and 5 m geogrid levels is related to the distribution of the maximum horizontal soil strains at the 0 m, 2 m and 4 m instrumentation levels. In the uniaxial geogrid slope, the 5 m geogrid level developed the largest strain while the 1 m level had the smallest. In the rectangular geogrid slope, the three geogrid levels developed maximum tensile strains of similar magnitude with a slightly higher strain occurring in the 3 m level.
5. During the four years after completion of the fill, no significant time-dependent strains were measured in either the uniaxial or the rectangular geogrids.
6. Settlement of the fill and the foundation soils developed as the fill was placed. Significant settlements and localized soil strains occurred only after the third and final construction season.
7. The development of the pore pressures in the fill and the foundation soils were closely related to the fill construction. The pore pressures increased as fill was placed during each construction season and dissipated when no fill was being placed. The rate of the dissipation decreased as fill height increased. The pore pressures measured in the fill were considerably larger than in the foundation soils. At each instrumentation location, the development of the pore pressure depended upon the overburden load and the degree of saturation of the embankment soil. The pore pressures at different locations tended to equilibrate between construction periods. The geogrid materials did not significantly affect the pore pressure magnitude and distribution within the fill.

ACKNOWLEDGEMENTS

Alberta Transportation and Utilities funded this research project. The assistance of colleagues at the University of Alberta and the assistance from the Geotechnical Section and the Research and Development Branch and District 7 of Alberta Transportation and Utilities is greatly appreciated.

REFERENCES

Bassett, R.H. and Yeo, K.C.,1988, "The Behavior of a Reinforced Trial Embankment on Soft Shallow Foundation", *Proceedings of the International Geotechnical Symposium on Theory and Practice of Earth Reinforcement,* Fukuoka, Kyushu, Japan, pp. 371-376.

Fannin, R.J. and Hermann, S., 1990, "Performance Data for a Sloped Reinforced Soil Wall", *Canadian Geotechnical Journal,* Vol. 27, No. 5, pp. 676-686.

Hofmann, B.A., 1989, "Evaluation of Soil Properties of the Devon Test Fill", M.Sc. Thesis, Department of Civil Engineering, University of Alberta, Edmonton, Alberta, Canada, 325 p.

Koerner, R.M., 1990, "Designing with Geosynthetics", 2nd Edition, Prentice Hall, New York, 652 p.

Liu, Y., 1992, "Performance of Geogrid Reinforced Clay Slopes", Ph. D. Thesis, Department of Civil Engineering, University of Alberta, Edmonton, Alberta, Canada, 406 p.

Mitchell, J.K., 1987, "Reinforcement for Earthwork Construction and Ground Stabilization", *Proceedings of the 8th Pan American Congress on Soil Mechanics and Foundation Engineering,* Cartagena, Columbia August, pp. 349-380.

Rimoldi, P., 1988, "A Review of Field Measurements of the Behavior of Geogrid Reinforced Slopes and Walls", *Proceedings of the International Geotechnical Symposium on Theory and Practice of Earth Reinforcement,* Fukuoka, Kyushu, Japan, pp. 571-576.

Sego, D.C., Scott, J.D., Richards, A.D. and Liu, Y., 1990 "Performance of a Geogrid in a Cohesive Soil Test Embankment", *Proceedings of the Fourth International Conference on Geotextiles, Geomembranes and Related Products,* Vol. 2, The Hague, The Netherlands, May 1990, pp. 67-72.